β^+ Gamow-Teller Strengths from Unstable ^{14}O via the $(d, {}^2\text{He})$ Reaction in Inverse Kinematics

S. Giraud[1,2,3,*] J. C. Zamora,[1] R. G. T. Zegers,[1,2,3,†] D. Bazin,[1,3] Y. Ayyad,[4,1] S. Bacca,[5,6] S. Beceiro-Novo,[3,7] B. A. Brown,[1,2,3] A. Carls,[1,2,3] J. Chen,[1,8] M. Cortesi,[1] M. DeNudt,[1,2,3] G. Hagen,[9,10] C. Hultquist,[1,2,3] C. Maher,[1,2,3] W. Mittig,[1,3] F. Ndayisabye,[1,2,3] S. Noji,[1] S. J. Novario,[9,10] J. Pereira,[1,2] Z. Rahman,[1,2,3] J. Schmitt,[1,2,3] M. Serikow,[1,2,3] L. J. Sun,[1,2] J. Surbrook,[1,2,3] N. Watwood,[1,2,3] and T. Wheeler[1,2,3]

[1]*Facility for Rare Isotope Beams, Michigan State University, East Lansing, Michigan 48824, USA*
[2]*Joint Institute for Nuclear Astrophysics: Center for the Evolution of the Elements, Michigan State University, East Lansing, Michigan 48824, USA*
[3]*Department of Physics and Astronomy, Michigan State University, East Lansing, Michigan 48824, USA*
[4]*IGFAE, Universidade de Santiago de Compostela, E-15782 Santiago de Compostela, Spain*
[5]*Institut für Kernphysik and PRISMA⁺ Cluster of Excellence, Johannes Gutenberg-Universität, 55128 Mainz, Germany*
[6]*Helmholtz-Institut Mainz, Johannes Gutenberg-Universität Mainz, D-55099 Mainz, Germany*
[7]*CITENI, Campus Industrial de Ferrol, Universidade da Coruña, Campus de Esteiro, 15403 Ferrol, Spain*
[8]*Physics Division, Argonne National Laboratory, Lemont, Illinois 60439, USA*
[9]*Physics Division, Oak Ridge National Laboratory, Oak Ridge, Tennessee 37831, USA*
[10]*Department of Physics and Astronomy, University of Tennessee, Knoxville, Tennessee 37996, USA*

For the first time, the $(d, {}^2\text{He})$ reaction was successfully used in inverse kinematics to extract the Gamow-Teller transition strength in the β^+ direction from an unstable nucleus. The new technique was made possible by the use of an active-target time-projection chamber and a magnetic spectrometer, and opens a path to addressing a range of scientific challenges, including in astrophysics and neutrino physics. In this Letter, the nucleus studied was ^{14}O, and the Gamow-Teller transition strength to ^{14}N was extracted up to an excitation energy of 22 MeV. The data were compared to shell-model and state-of-the-art coupled-cluster calculations. Shell-model calculations reproduce the measured Gamow-Teller strength distribution up to about 15 MeV reasonably well, after the application of a phenomenological quenching factor. In a significant step forward to better understand this quenching, the coupled-cluster calculation reproduces the full strength distribution well without such quenching, owing to the large model space, the inclusion of strong correlations, and the coupling of the weak interaction to two nucleons through two-body currents.

Nuclear charge-exchange (CE) reactions provide important tools for studying the spin-isospin response of nuclei and provide important information about nuclear structure, bulk properties of nuclei, and processes mediated by the weak nuclear force [1–8]. Of particularly high impact has been the ability to indirectly and model-independently extract Gamow-Teller (GT) transitions strength from CE experiments at intermediate beam energies ($E \gtrsim 100$ MeV/ nucleon). GT transitions are associated with the transfer of spin ($\Delta S = 1$), isospin ($\Delta T = 1$), and no angular momentum ($\Delta L = 0$), and mediate allowed β decay and electron captures (ECs). The latter play important roles in astrophysical phenomena [5,8], such as core-collapse supernovae [9–11], thermonuclear supernovae [12,13], and the crusts of neutron stars that accrete material from binary-system companions [14,15].

The extraction of the GT transition strengths [$B(\text{GT})$] from CE reactions, which are mediated by the strong nuclear force, is possible because of the well-established proportionality between the extracted differential cross section at small momentum transfer ($q \approx 0$) and $B(\text{GT})$ [16], valid for $B(\text{GT}) \gtrsim 0.01$ [17]. The proportionality factor, referred to as the unit cross section ($\hat{\sigma}_{\text{GT}}$), is conveniently calibrated using transitions for which the $B(\text{GT})$ is known directly from β/EC decay. Unlike β/EC decay, the extraction of $B(\text{GT})$ from CE experiments is not limited to a finite Q-value window, which is important for the astrophysical applications, where, due to high stellar temperatures and/or densities, EC transitions to highly excited states can occur. For constraining the astrophysical EC rates, charge-exchange reactions in the (n, p) direction are key.

In the astrophysical scenarios mentioned above, ECs on many unstable isotopes play crucial roles. Compared to (p, n) CE reactions, for which experiments in inverse kinematics (i.e., with the unstable nucleus of interest being produced as the beam) were successfully performed to study GT transitions in the β^- direction up to high

excitation energy (E_x) and across the chart of isotopes [18–27], the development of CE experiments in the (n, p) direction in inverse kinematics with beams of unstable isotopes has been more challenging. The $(^7\text{Li}, ^7\text{Be} + \gamma)$ reaction was successfully developed to study (n, p)-type CE reactions in inverse kinematics [28,29], but it can only be used for light ($A \lesssim 35$) nuclei and low E_x. In this Letter, we present the successful development of an alternative method, namely, the $(d, ^2\text{He})$ reaction in inverse kinematics, which can be used to extract $B(\text{GT})$ up to high E_x and without intrinsic limitations on the mass of the isotope.

In the first experiment presented here, Gamow-Teller transitions from unstable ^{14}O to ^{14}N were studied to extract the GT strength distribution for $E_x \lesssim 22$ MeV. The measurement complements previous studies in the $A = 14$ multiplet [30–37]. The $A = 14$ nuclei have posed significant challenges to theoretical calculations and require the inclusion of three-body forces and an accurate treatment of two-body currents (2BCs), for example, to explain the anomalously long half-lives (corresponding to very small GT transition strengths) for the analog β decays from ^{14}O and ^{14}C to ground state (g.s.) of ^{14}N [38–41]. In recent effective field theory (EFT) calculations [42], it is possible to explain, based on first principles, the reduction of GT strength observed in experimental data compared to other theoretical calculations, including the shell model (SM). This reduction, referred to as the "quenching" of the GT strength [43–45], has important implications for the astrophysical applications, such as the ones mentioned above, as well as fundamental phenomena such as neutrinoless double-β decay [46,47]. By including strong correlations present in the nucleus and the coupling of the weak interaction to two nucleons through two-body currents in addition to the one-body Gamow-Teller operator, it is possible to describe the quenching in the EFT calculations [42,48]. It is important to further test such calculations by comparing GT transition strength up to high E_x, including for nuclei far from stability. Charge-exchange reactions in inverse kinematics, and the $(d, ^2\text{He})$ reaction in particular, are excellent tools for this purpose.

The $(d, ^2\text{He})$ reaction in forward kinematics, i.e., with a deuteron beam, has been used to study many stable nuclei [49–52]. The $(d, ^2\text{He})$ reaction refers to a $(d, 2p)$ reaction for which the two outgoing protons couple to a $^1S_0$ ($T = 1$) state. This state is unbound by ≈ 0.5 MeV. Contributions from higher partial waves become significant at higher internal energy $\epsilon_{pp} \gtrsim 4$ MeV [53]. The wave function of the deuteron is dominated by the $^3S_1$ ($T = 0$) configuration. Therefore, the $(d, ^2\text{He})$ reaction at low ^2He internal energy ($\epsilon_{pp} \lesssim 2$ MeV) is selective to excitations involving the transfer of spin ($\Delta S = 1$) [49,53]. In inverse kinematics, and for $(d, ^2\text{He})$ reactions at $q \approx 0$, the energy of the two protons emitted is very small, making the use of a foil (e.g., CD_2) or liquid deuterium unfeasible. Therefore, a gaseous active-target time-projection chamber (ATTPC)

[54] was used in the present work, in which the deuterium gas served as both the target and the tracking medium for the protons. The beamlike fragment (i.e., ^{14}N, or one of its decay products) was detected in the S800 spectrograph [55] to serve as a trigger for CE events.

A 10- to 50-pnA, 150-MeV/nucleon beam of ^{16}O was accelerated by the Coupled Cyclotron Facility at the National Superconducting Cyclotron Laboratory (NSCL), and struck a 1316-mg/cm^2-thick Be production target. A 150-mg/cm^2-thick Al degrader was used in the A1900 fragment separator [56] to produce a 70%-pure ^{14}O beam at 105 MeV/nucleon and with intensities between 0.2 and 0.7 Mpps. The time-of-flight (TOF) between two scintillators placed at the exit of the A1900 and the entrance of the S800 spectrograph [55] beam line (the S800 object point) was used to separate ^{14}O from ^{13}N (23%) and ^{12}C (7%) contaminants on an event-by-event basis. The ATTPC [54], used for the first time with a fast rare-isotope beam, was filled with pure deuterium gas at a pressure of 530 Torr ($\pm 0.5\%$), corresponding to a thickness of 11.7 mg/cm^2. The gas of the active volume was isolated from the beam line and S800 vacuum by 12-μm-thick polyamide windows. In the ATTPC, a 500-V/cm uniform electric field, directed along the beam axis, drifts electrons produced by ionizing charged particles upstream toward a micromegas pad plane with 10 240 independent readout channels, which provides the transverse track images. The third position coordinate, along the beam direction, is determined from the drift time of the electrons. The drift velocity was ≈ 0.9 cm/μs. The pad plane has a central aperture of 3-cm diameter to allow the beam to enter the ATTPC. Hence, tracks from the beam particles and outgoing beamlike fragments are not observed in the ATTPC. The fragment identification was performed event by event using the TOF between scintillators at the S800 object point and at the focal plane of S800, and the energy loss of the fragments in an ionization chamber at the focal plane of S800. The object scintillator was also used to monitor the beam rate for the cross-section determination and the focal plane scintillator was used to trigger a ≈ 110-μs-long readout window for signals from the ATTPC. Momenta of the fragments at the target were reconstructed from the positions and angles measured with two cathode-readout drift chambers [57] at the S800 focal plane. These reconstructed quantities were used for S800 acceptance corrections and determining absolute cross sections.

The excitation energy of ^{14}N produced after the $^{14}\text{O}(d, ^2\text{He})$ reaction is reconstructed in three steps. First, the electron cloud produced by ionizing charged particles in the ATTPC is analyzed with pattern recognition and fitting routines to identify the $(d, ^2\text{He})$ events and extract the ^2He momentum [58,59]. The selection of $(d, ^2\text{He})$ events is ensured by the coincidence between an identified ^{14}O ion in the beam, a relevant residual fragment in the S800, and two fitted tracks with a minimal distance smaller than 2σ of the

minimal-distance distribution ($\lesssim 1$ cm) in the beam region. The point of minimal distance defines the reaction vertex. The energy (deduced from the range) and angular resolutions of a single track are about 15 keV and 1.5°, respectively. The momentum vectors of the two protons are used to reconstruct the ^{2}He momentum vector and, through an invariant-mass calculation, its internal energy. Finally, the excitation energy of ^{14}N is obtained from a missing-mass calculation.

Simulations for estimating the efficiency and acceptance of the experiment were performed with the ATTPCROOT package [60–62], using a $(d, ^2\text{He})$ event generator based on calculated cross sections using the code adiabatic coupled-channels Born approximation ACCBA [50,63], specifically developed for $(d, ^2\text{He})$ reactions. The code reproduces well the differential cross sections for $(d, ^2\text{He})$ reactions performed in forward kinematics [64,65]. For the entrance and exit channels, optical-model parameters obtained from the Koning-Delaroche phenomenological potential [66] for protons and deuterons (extended parametrization in the code TALYS [67,68]) were used. The Love-Franey effective nucleon-nucleon interaction at 140 MeV [69] was used. The spectroscopic amplitudes of the transitions were obtained from SM calculations in the p-shell model space and the CKII [70] interaction using the NUSHELLX [71] code. In the ATTPCROOT simulation the analog signal of each pad of the sensor plane is analyzed in the same manner as the experimental data and the reconstruction of the simulated events is performed with the same algorithms as for the experimental data. Therefore, the simulation also provides realistic estimations of the efficiency and acceptance of the ATTPC.

Figure 1(a) shows the extracted differential cross sections as a function of the $E_x(^{14})$N at scattering angles below 8° gated on ^{14}N, or its decay products (^{13}C, ^{13}N, ^{12}C, and ^{10}B) identified with the S800 for E_x above the ^{14}N particle-decay thresholds, as indicated. The experimental spectra are almost background-free due to the stringent conditions for the event selection. Note that these spectra are integrated over the ϵ_{pp} range accepted by the ATTPC. At small scattering angles and small reaction Q value, the two protons have the lowest energies, requiring ϵ_{pp} to be within 1.5 and 2.5 MeV for both protons to escape the central insensitive region and not leave the chamber. At larger scattering angles and Q values, only events with $\epsilon_{pp} < 1$ MeV have path lengths that end inside the ATTPC and can be reconstructed. Figure 1(b) shows the total differential cross sections for scattering angles below 3°. Near $Q = 0$ ($E_x = 3.7$ MeV), E_x is almost completely determined by the angle of the reconstructed ^{2}He particle, and the resolution is limited to ∼2.1 MeV full width at half maximum value (FWHM). At smaller and larger Q values, the energy of the ^{2}He particle is also important, and a resolution of ∼1.2 MeV can be achieved.
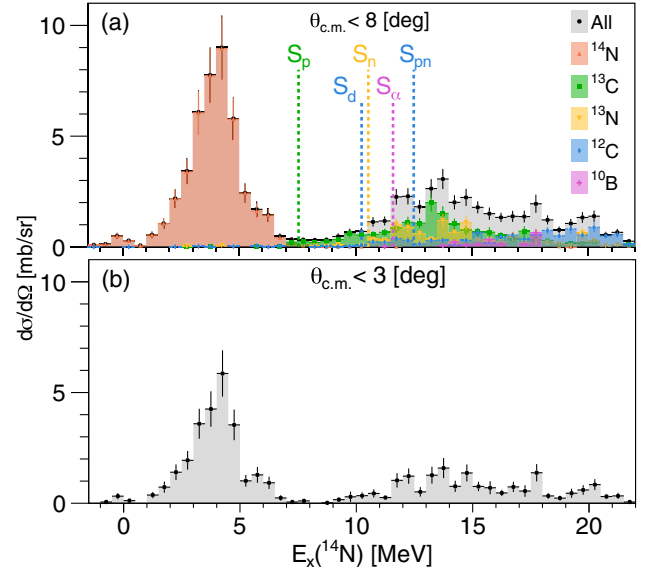

FIG. 1. Differential cross sections for the $^{14}\text{O}(d, ^2\text{He})$ reaction (a) for the entire scattering angle range ($\theta_{\text{c.m.}} < 8°$) and (b) for $\theta_{\text{c.m.}} < 3°$. In (a) the colors represent the contributions from the different decay channels corresponding to respective fragments detected in the S800 spectrometer, and the vertical dashed lines indicates the ^{14}N particle-decay thresholds ($S_p = 7.55$ MeV, $S_n = 10.55$ MeV, $S_d = 10.26$ MeV, $S_\alpha = 11.61$ MeV, and $S_{pn} = 12.50$ MeV).

Figure 2 shows the differential cross sections for different E_x regions. The error bars in the data include statistical and systematic uncertainties. The latter are dominated by uncertainties in the acceptance corrections and beam-intensity determination, but are relatively small compared to the statistical uncertainties, except for the state at 3.95 MeV, for which both types of uncertainty are comparable. In order to extract the $\Delta L = 0$ (GT) contributions from the E_x spectra, a multipole decomposition analysis (MDA) [72,73] was performed. Two analyses were performed: one in which the MDA was done for E_x bins of 3-MeV wide and one in which the E_x regions were adjusted to localize regions with significant and insignificant GT contributions, also making use of $^{14}\text{C}(p, n)$ data [34–36]. We present the results from the latter method, as it best localizes the GT strength. For each region, the experimental differential cross sections were fitted with a linear combination of calculated angular distributions associated with angular momentum transfers $\Delta L = 0$, 1, and 2. The lower the angular momentum transfers are, the more forward peaked the differential cross sections are. Transitions with $\Delta L > 2$ are suppressed near $q = 0$ and are not included in the fit, but minor contributions might be absorbed in the extracted components with $\Delta L = 1$ and 2. Prior to the fit, the calculated differential cross sections for each ΔL from ACCBA were inserted in the ATTPCROOT simulation to account for the ϵ_{pp} acceptance of the ATTPC as a function
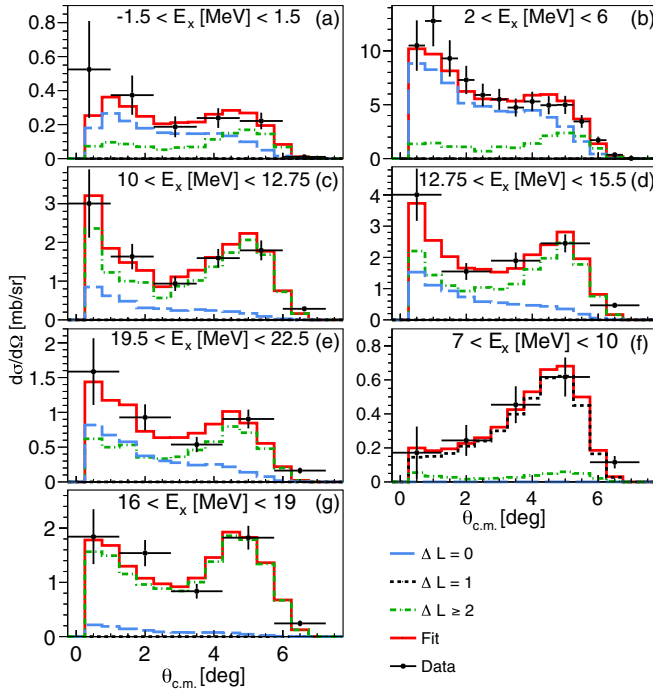
FIG. 2. Differential cross sections at different E_x with MDA results, using angular distributions from the ATTPCROOT simulation. Panels (a)–(e) are gated on E_x ranges with peaks; see Fig. 1. Panels (f) and (g) are gated on regions without strong GT transition.

of scattering angle and Q value, as discussed above. The MDA results are shown in Fig. 2 as colored histograms.

The dominant peak in the spectra of Fig. 1 is the transition to the 1^+ state at 3.95 MeV, which has a known $B(GT)$ of 2.73 from β decay [37]. As expected for a strong GT transition, it is dominated by $\Delta L = 0$, as shown in Fig. 2(b). The 0^+ isobaric analog of the ^{14}O g.s. at 2.31 MeV is not notably excited, as expected for the $\Delta S = 1$ $(d, {}^2\text{He})$ reaction and unlike the case for the isospin-symmetric ^{14}C(p, n) reaction [34–36].

To compare the unit cross section [16] from the present experiment with that obtained from previous $(d, {}^2\text{He})$ experiments in forward kinematics [64], the $\Delta L = 0$ fraction of the cross section obtained after MDA was extrapolated to $\epsilon_{pp} < 1$ MeV and $q = 0$ on the basis of the ACCBA calculations. A unit cross section of $\hat{\sigma}_{GT} = 2.74 \pm 0.29$ mb/sr was obtained, in good agreement with the value of 2.58 ± 0.14 mb/sr found for the ^{12}C$(d, {}^2\text{He})$ reaction in forward kinematics [64] at a beam energy of 85 MeV/nucleon, giving confidence in the determination of the absolute cross sections in the present experiment performed in inverse kinematics.

Additional GT strength was identified in the E_x regions between 10–12.75 MeV [Fig. 2(c)], 12.75–15.5 MeV [Fig. 2(d)], and 19.5–22.5 MeV [Fig. 2(e)]. The associated $B(GT)$s were extracted by using the $\hat{\sigma}_{GT}$ obtain from the state at 3.95 MeV, as shown in Fig. 3. The other regions had

$B(GT)$s consistent with 0. As examples, the MDA for the regions between 7–10 MeV and 16–19 MeV are shown in Figs. 2(f) and 2(g), indicating the dominance of transitions with $\Delta L > 0$. The GT strengths observed in the regions between 10–12.75 MeV and 12.75–15.5 MeV most likely correspond to 1^+ states observed at 11.5 and 13.75 MeV in the isospin-symmetric ^{14}C(p, n) reaction [34–36], populating the same states in ^{14}N. The summed strengths for these two states are very similar in the $(d, {}^2\text{He})$ and analog (p, n) experiments. The GT strength observed between 19.5 and 22.5 MeV was not observed in the ^{14}C(p, n) experiments. Unlike the latter experiments, in which contributions from the ^{12}C(p, n) reaction ($Q = -18.1$ MeV) due to ^{12}C contaminants in the target made extraction of GT strength for the ^{14}C(p, n) reaction ($Q = -0.626$ MeV) difficult, the present result has no background and the higher-lying strength was unambiguously identified.

The transition to the ^{14}N ground state is special. The known $B(GT)$ of 2×10^{-4} from ^{14}O β decay [37,74] is well below the value for which the proportionality between $B(GT)$ and the CE cross section holds [16,17]. The ^{14}O$(d, {}^2\text{He})^{14}$N(g.s.) measured cross section associated with $\Delta L = 0$ at $0°$ is more than 100 times larger than expected based on the $B(GT)$, which is comparable with the results from the ^{14}N$({}^3\text{He}, t)^{14}$O(g.s.) [32] and the analog ^{14}C$(p, n)^{14}$N(g.s.) [16] reactions. To accurately describe the properties of this very weak transition, a consistent inclusion of two- and three-body (NN + 3N) forces and 2BCs is necessary [41]. In the remainder of the analysis, the $B(GT)$ extracted from β decay was used, including in Fig. 3.

To test our understanding of the measured GT strength distribution, we compare with the SM calculations discussed above after applying a phenomenological quenching factor
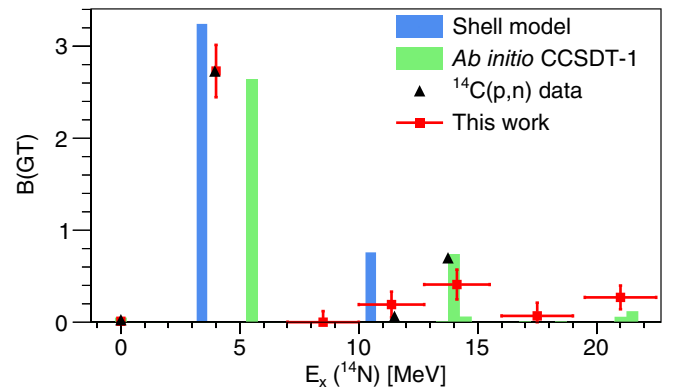

FIG. 3. Comparison between the $B(GT)$ distribution obtained from the present ^{14}O$(d, {}^2\text{He})$ experiment, the analog ^{14}C(p, n) reaction at $E_p = 160$ MeV [34], and theory by using SM and CC calculations (for details, see text). The horizontal error bars in the experimental data points from this Letter correspond to the regions in which the GT strength was observed and extracted from the MDA analysis.

of 0.67 [75] and a coupled-cluster (CC) calculation in which the same NN + 3N interaction and 2BCs of Ref. [42] are used. We include effects of 2BCs by multiplying the one-body GT strength by a factor from the Ikeda sum rule in Ref. [42] (similar to the method in Ref. [76]), which amounts to a reduction in GT strength by a factor of 0.82. Please note that, since the $B(\mathrm{GT})$ extracted from the CE data is calibrated to β decay as discussed above, the effects of 2BCs are, effectively, also included in the extracted strengths. The CC calculation was performed using a natural orbital [77] Hartree-Fock basis built from 15 major spherical oscillator shells with a frequency of $\hbar\omega = 16$ MeV. We employed the chiral potential 1.8/2.0 (EM) [78] with 3N forces normal ordered to the two-body level [79]. With this basis, the non-Hermitian CC effective Hamiltonian was computed by solving the ^{14}O ground state, which was used in turn to compute the corresponding left ground state [80,81]. The Gamow-Teller response function was then computed using the equation-of-motion method for excited states [82] and the Lanczos continued fraction method [83]. Both the ground and excited states were truncated at the singles, doubles, and approximate triples level (method CCSDT-1) [84].

The comparisons between the experimental data and theory are shown in Fig. 3. Overall, the theoretical calculations match the experimental data quite well. Aside from the transition to the ground state, the CC calculations put the strength at slightly higher E_x than the SM calculations, with the latter doing better for the strong transition to the 3.97-MeV state, and the CC calculation being more accurate for the strength between 10 and 15 MeV. In the present experiment, GT strength is found at ~21 MeV. In contrast to the SM calculation, the CC calculations reproduce this strength, owing to the large model space used. The summed experimental GT strength up to 22 MeV is $\Sigma B(\mathrm{GT}) = 3.69 \pm 0.75$, consistent with the CC calculations [$\Sigma B(\mathrm{GT}) = 3.71$] and the SM calculations after quenching [$\Sigma B(\mathrm{GT}) = 4.02$].

In summary, we have demonstrated that the $(d, {}^2\mathrm{He})$ reaction at ~100 MeV/nucleon in inverse kinematics by using an active-target time-projection chamber placed in front of a magnetic spectrometer is an excellent method for model-independently extracting Gamow-Teller transition strengths in the β^+ direction from unstable nuclei. We applied this method for the first time to extract the GT strength distribution from ^{14}O and used it to test state-of-the-art CC calculations that take into consideration three-nucleon force and 2BCs. In comparison with the SM, the CC calculations do not require a phenomenological quenching factor to reproduce the experimental strength distribution. By using the same experimental method, similar detailed tests of theoretical models can be performed far from the valley of stability. This is not only of interest for testing *ab initio* nuclear theories, but also to test a wider range of theoretical models, such as shell models and density-functional theories, which are necessary for efficiently estimating GT transition strength in the β^+/EC direction for a large number of nuclei. Such efforts will, for example, be important for estimating electron-capture rates in astrophysical scenarios. In combination with the previous development of the (p, n) reaction in inverse kinematics [24], experimental methods to use charge-exchange reactions to probe GT transition strengths from unstable nuclei beyond the Q-value window accessible through direct measurements of β/EC decay are now available in both β^+ and β^- directions.

---

*giraud@frib.msu.edu
†zegers@frib.msu.edu

[1] F. Osterfeld, Rev. Mod. Phys. **64**, 491 (1992).
[2] J. Rapaport and E. Sugarbaker, Annu. Rev. Nucl. Part. Sci. **44**, 109 (1994).

[3] M. N. Harakeh and A. Woude, *Giant Resonances: Fundamental High-Frequency Modes of Nuclear Excitation* (Oxford University Press on Demand, New York, 2001), Vol. 24.

[4] M. Ichimura, H. Sakai, and T. Wakasa, Prog. Part. Nucl. Phys. **56**, 446 (2006).

[5] K. Langanke and G. Martínez-Pinedo, Rev. Mod. Phys. **75**, 819 (2003).

[6] Y. Fujita, B. Rubio, and W. Gelletly, Prog. Part. Nucl. Phys. **66**, 549 (2011).

[7] D. Frekers and M. Alanssari, Eur. Phys. J. **54**, 177 (2018).

[8] K. Langanke, G. Martínez-Pinedo, and R. G. T. Zegers, Rep. Prog. Phys. **84**, 066301 (2021).

[9] H. Bethe, G. Brown, J. Applegate, and J. Lattimer, Nucl. Phys. **A324**, 487 (1979).

[10] G. M. Fuller, W. A. Fowler, and M. J. Newman, Astrophys. J. Suppl. Ser. **48**, 279 (1982).

[11] H.-T. Janka, K. Langanke, A. Marek, G. Martínez-Pinedo, and B. Müller, Phys. Rep. **442**, 38 (2007).

[12] F. Brachwitz, D. J. Dean, W. R. Hix, K. Iwamoto, K. Langanke, G. Martínez-Pinedo, K. Nomoto, M. R. Strayer, F. Thielemann, and H. Umeda, Astrophys. J. **536**, 934 (2000).

[13] K. Iwamoto, F. Brachwitz, K. Nomoto, N. Kishimoto, H. Umeda, W. R. Hix, and F. Thielemann, Astrophys. J. Suppl. Ser. **125**, 439 (1999).

[14] H. Schatz, S. Gupta, P. Möller, M. Beard, E. F. Brown, A. T. Deibel, L. R. Gasques, W. R. Hix, L. Keek, R. Lau et al., Nature (London) **505**, 62 (2014).

[15] P. Haensel and J. L. Zdunik, Astron. Astrophys. **227**, 431 (1990).

[16] T. Taddeucci, C. Goulding, T. Carey, R. Byrd, C. Goodman, C. Gaarde, J. Larsen, D. Horen, J. Rapaport, and E. Sugarbaker, Nucl. Phys. **A469**, 125 (1987).

[17] R. G. T. Zegers, H. Akimune, S. M. Austin, D. Bazin, A. M. vandenBerg, G. P. A. Berg, B. A. Brown, J. Brown, A. L. Cole, I. Daito et al., Phys. Rev. C **74**, 024309 (2006).

[18] M. D. Cortina-Gil, P. Roussel-Chomaz, N. Alamanos, J. Barrette, W. Mittig, F. Auger, Y. Blumenfeld, J. M. Casandjian, M. Chartier, V. Fekou-Youmbi et al., Phys. Lett. B **371**, 14 (1996).

[19] J. A. Brown, D. Bazin, W. Benenson, J. Caggiano, M. Fauerbach, M. Hellström, J. H. Kelley, R. A. Kryger, R. Pfaff, B. M. Sherrill et al., Phys. Rev. C **54**, R2105 (1996).

[20] S. Shimoura, T. Teranishi, Y. Ando, M. Hirai, N. Iwasa, T. Kikuchi, S. Moriya, T. Motobayashi, T. Murakami, T. Nakamura et al., Nucl. Phys. **A616**, 208 (1997).

[21] T. Teranishi, S. Shimoura, Y. Ando, M. Hirai, N. Iwasa, T. Kikuchi, S. Moriya, T. Motobayashi, H. Murakami, T. Nakamura et al., Phys. Lett. B **407**, 110 (1997).

[22] S. Takeuchi, S. Shimoura, T. Motobayashi, H. Akiyoshi, Y. Ando, N. Aoi, Z. Fü, T. Gomi, Y. Higurashi, M. Hirai et al., Phys. Lett. B **515**, 255 (2001).

[23] Z. Li, W. Liu, X. Bai, Y. Wang, G. Lian, Z. Li, and S. Zeng, Phys. Lett. B **527**, 50 (2002).

[24] M. Sasano, G. Perdikakis, R. G. T. Zegers, S. M. Austin, D. Bazin, B. A. Brown, C. Caesar, A. L. Cole, J. M. Deaven, N. Ferrante et al., Phys. Rev. Lett. **107**, 202501 (2011).

[25] J. Yasuda, M. Sasano, R. G. T. Zegers, H. Baba, D. Bazin, W. Chao, M. Dozono, N. Fukuda, N. Inabe, T. Isobe et al., Phys. Rev. Lett. **121**, 132501 (2018).

[26] M. Kobayashi, K. Yako, S. Shimoura, M. Dozono, N. Fukuda, N. Inabe, D. Kameda, S. Kawase, K. Kisamori, T. Kubo et al., JPS Conf. Proc 030089 (2015).

[27] S. I. Lipschutz, The (p, n) charge-exchange reaction in inverse kinematics as a probe for isovector giant resonances in exotic nuclei, Ph.D. thesis, Michigan State University, East Lansing, Michigan, 2018, 10.25335/M5G29H.

[28] R. G. T. Zegers, R. Meharchand, Y. Shimbara, S. M. Austin, D. Bazin, B. A. Brown, C. A. Diget, A. Gade, C. J. Guess, M. Hausmann et al., Phys. Rev. Lett. **104**, 212504 (2010).

[29] R. Meharchand, R. G. T. Zegers, B. A. Brown, S. M. Austin, T. Baugher, D. Bazin, J. Deaven, A. Gade, G. F. Grinyer, C. J. Guess et al., Phys. Rev. Lett. **108**, 122501 (2012).

[30] W. R. Wharton, C. D. Goodman, and D. C. Hensley, Phys. Rev. C **22**, 1138 (1980).

[31] N. Anantaraman, J. S. Winfield, S. M. Austin, A. Galonsky, J. van der Plicht, C. C. Chang, G. Ciangaru, and S. Gales, Phys. Rev. Lett. **57**, 2375 (1986).

[32] A. Negret, T. Adachi, B. R. Barrett, C. Bäumer, A. M. van den Berg, G. P. A. Berg, P. von Brentano, D. Frekers, D. De Frenne, H. Fujita et al., Phys. Rev. Lett. **97**, 062502 (2006).

[33] F. Ajzenberg-Selove, Nucl. Phys. **A523**, 1 (1991).

[34] C. Goodman, C. Foster, D. Bainum, C. Gaarde, J. Larsen, C. Goulding, D. Horen, T. Masterson, J. Rapaport, T. Taddeucci, and E. Sugarbaker, Annual Scientific and Technical Report, Indiana University Cyclotron Facility, 1980, p. 44.

[35] T. N. Taddeucci, T. A. Carey, C. Gaarde, J. Larsen, C. D. Goodman, D. J. Horen, T. Masterson, J. Rapaport, T. P. Welch, and E. Sugarbaker, Phys. Rev. Lett. **52**, 1960 (1984).

[36] J. Rapaport, D. Wang, J. A. Carr, F. Petrovich, C. C. Foster, C. D. Goodman, C. Gaarde, J. Larsen, C. A. Goulding, T. N. Taddeucci et al., Phys. Rev. C **36**, 500 (1987).

[37] A. M. Hernandez and W. W. Daehnick, Phys. Rev. C **24**, 2235 (1981).

[38] P. Maris, J. P. Vary, P. Navrátil, W. E. Ormand, H. Nam, and D. J. Dean, Phys. Rev. Lett. **106**, 202502 (2011).

[39] J. W. Holt, G. E. Brown, T. T. S. Kuo, J. D. Holt, and R. Machleidt, Phys. Rev. Lett. **100**, 062501 (2008).

[40] J. W. Holt, N. Kaiser, and W. Weise, Phys. Rev. C **79**, 054331 (2009).

[41] A. Ekström, G. R. Jansen, K. A. Wendt, G. Hagen, T. Papenbrock, S. Bacca, B. Carlsson, and D. Gazit, Phys. Rev. Lett. **113**, 262504 (2014).

[42] P. Gysbers, G. Hagen, J. D. Holt, G. R. Jansen, T. D. Morris, P. Navrátil, T. Papenbrock, S. Quaglioni, A. Schwenk, S. R. Stroberg, and K. A. Wendt, Nat. Phys. **15**, 428 (2019).

[43] I. Towner, Phys. Rep. **155**, 263 (1987).

[44] C. Gaarde, J. Rapaport, T. Taddeucci, C. Goodman, C. Foster, D. Bainum, C. Goulding, M. Greenfield, D. Hören, and E. Sugarbaker, Nucl. Phys. **A369**, 258 (1981).

[45] B. A. Brown and B. H. Wildenthal, Annu. Rev. Nucl. Part. Sci. **38**, 29 (1988).

[46] J. Engel and J. Menéndez, Rep. Prog. Phys. **80**, 046301 (2017).

[47] J. T. Suhonen, Front. Phys. **5**, 55 (2017).

[48] G. B. King, L. Andreoli, S. Pastore, M. Piarulli, R. Schiavilla, R. B. Wiringa, J. Carlson, and S. Gandolfi, Phys. Rev. C **102,** 025501 (2020).

[49] H. Ohnuma, K. Hatanaka, S. I. Hayakawa, M. Hosaka, T. Ichihara, S. Ishida, S. Kato, T. Niizeki, M. Ohura, H. Okamura *et al.*, Phys. Rev. C **47,** 648 (1993).

[50] H. Okamura, S. Fujita, Y. Hara, K. Hatanaka, T. Ichihara, S. Ishida, K. Katoh, T. Niizeki, H. Ohnuma, H. Otsu *et al.*, Phys. Lett. B **345,** 1 (1995).

[51] H. M. Xu, G. K. Ajupova, A. C. Betker, C. A. Gagliardi, B. Kokenge, Y.-W. Lui, and A. F. Zaruba, Phys. Rev. C **52,** R1161 (1995).

[52] D. Frekers, Nucl. Phys. **A731,** 76 (2004).

[53] S. Kox, J. Carbonell, C. Furget, T. Motobayashi, C. Perrin, C. Wilkin, J. Arvieux, J. Bocquet, A. Boudard, G. Gaillard *et al.*, Nucl. Phys. **A556,** 621 (1993).

[54] J. Bradt, D. Bazin, F. Abu-Nimeh, T. Ahn, Y. Ayyad, S. B. Novo, L. Carpenter, M. Cortesi, M. Kuchera, W. Lynch *et al.*, Nucl. Instrum. Methods Phys. Res., Sect. B **875,** 65 (2017).

[55] D. Bazin, J. Caggiano, B. Sherrill, J. Yurkon, and A. Zeller, Nucl. Instrum. Methods Phys. Res., Sect. B **204,** 629 (2003).

[56] D. Morrissey, B. Sherrill, M. Steiner, A. Stolz, and I. Wiedenhoever, Nucl. Instrum. Methods Phys. Res., Sect. B **204,** 90 (2003).

[57] J. Yurkon, D. Bazin, W. Benenson, D. Morrissey, B. Sherrill, D. Swan, and R. Swanson, Nucl. Instrum. Methods Phys. Res., Sect. B **422,** 291 (1999).

[58] Y. Ayyad, W. Mittig, D. Bazin, S. Beceiro-Novo, and M. Cortesi, Nucl. Instrum. Methods Phys. Res., Sect. A **880,** 166 (2018).

[59] J. Zamora and G. Fortino, Nucl. Instrum. Methods Phys. Res., Sect. A **988,** 164899 (2021).

[60] Y. Ayyad, W. Mittig, D. Bazin, and M. Cortesi, J. Phys. Conf. Ser. **876,** 012003 (2017).

[61] Y. Ayyad, ATTPCROOT, https://github.com/ATTPC/ ATTPCROOTv2.

[62] S. Giraud, J. Zamora, R. Zegers, Y. Ayyad, D. Bazin, W. Mittig, A. Carls, M. DeNudt, and Z. Rahman, Nucl. Instrum. Methods Phys. Res., Sect. A **1051,** 168213 (2023).

[63] H. Okamura, Phys. Rev. C **60,** 064602 (1999).

[64] S. Rakers, C. Bäumer, D. Frekers, R. Schmidt, A. M. van den Berg, V. M. Hannen, M. N. Harakeh, M. A. de Huu, H. J. Wörtche, D. De Frenne *et al.*, Phys. Rev. C **65,** 044323 (2002).

[65] E. W. Grewe, C. Bäumer, A. M. van den Berg, N. Blasi, B. Davids, D. De Frenne, D. Frekers, P. Haefner, M. N. Harakeh, M. Huynyadi *et al.*, Phys. Rev. C **69,** 064325 (2004).

[66] A. Koning and J. Delaroche, Nucl. Phys. **A713,** 231 (2003).

[67] A. J. Koning, S. Hilaire, and M. C. Duijvestijn, in *Proceedings of the International Conference on Nuclear Data for Science and Technology* (2007), pp. 211–214.

[68] A. Koning and D. Rochman, Nucl. Data Sheets **113,** 2841 (2012).

[69] M. A. Franey and W. G. Love, Phys. Rev. C **31,** 488 (1985).

[70] S. Cohen and D. Kurath, Nucl. Phys. **73,** 1 (1965).

[71] B. Brown and W. Rae, Nucl. Data Sheets **120,** 115 (2014).

[72] B. Bonin, N. Alamanos, B. Berthier, G. Bruge, H. Faraggi, D. Legrand, J. Lugol, W. Mittig, L. Papineau, A. Yavin *et al.*, Nucl. Phys. **A430,** 349 (1984).

[73] M. Moinester, A. Trudel, K. Raywood, S. Yen, B. Spicer, R. Abegg, W. Alford, N. Auerbach, A. Celler, D. Frekers *et al.*, Phys. Lett. B **230,** 41 (1989).

[74] H. S. Wilson, R. W. Kavanagh, and F. M. Mann, Phys. Rev. C **22,** 1696 (1980).

[75] W.-T. Chou, E. K. Warburton, and B. A. Brown, Phys. Rev. C **47,** 163 (1993).

[76] S. Novario, P. Gysbers, J. Engel, G. Hagen, G. R. Jansen, T. D. Morris, P. Navrátil, T. Papenbrock, and S. Quaglioni, Phys. Rev. Lett. **126,** 182502 (2021).

[77] A. Tichai, J. Müller, K. Vobig, and R. Roth, Phys. Rev. C **99,** 034321 (2019).

[78] K. Hebeler, S. K. Bogner, R. J. Furnstahl, A. Nogga, and A. Schwenk, Phys. Rev. C **83,** 031301(R) (2011).

[79] G. Hagen, T. Papenbrock, D. J. Dean, A. Schwenk, A. Nogga, M. Włoch, and P. Piecuch, Phys. Rev. C **76,** 034302 (2007).

[80] R. J. Bartlett and M. Musiał, Rev. Mod. Phys. **79,** 291 (2007).

[81] G. Hagen, T. Papenbrock, M. Hjorth-Jensen, and D. J. Dean, Rep. Prog. Phys. **77,** 096302 (2014).

[82] J. F. Stanton and R. J. Bartlett, J. Chem. Phys. **98,** 7029 (1993).

[83] M. Miorelli, S. Bacca, N. Barnea, G. Hagen, G. R. Jansen, G. Orlandini, and T. Papenbrock, Phys. Rev. C **94,** 034317 (2016).

[84] J. D. Watts and R. J. Bartlett, Chem. Phys. Lett. **233,** 81 (1995).